ISSUES IN MODELLING OF NEGATIVE ION EXTRACTION

M. Cavenago *, INFN-LNL, Legnaro, Italy; V. Antoni, F. Sattin, Consorzio RFX, Padova, Italy

Abstract

The classical Tonks-Langmuir one dimensional (1D) free fall ion model of sheath is adapted and generalized to two dimensional (2D) geometries, giving a rigorous base to ion tracing codes. The reduction of integro-differential equations to a coupled system of partial differential equation (PDE), suitable for 2D applications, is performed. The distinction between plasma core and frontal plasma is naturally introduced. Numerical results of this model (still limited to positive ion case for simplicity) and comparisons with an ad hoc developed tracing code are given.

INTRODUCTION

In the context of negative ion sources proposed for neutral beam injectors (NBI) for tokamaks, halo of the extracted beam is large (typically 10 %) and optimum shape of the multiaperture plasma grid electrode (PG) is a matter of experimental and theoretical research. Halo depends on electrode edges and on the nearby distortion of the charge sheath layer, so that this article discusses preliminary issues of sheath modelling in 2D.

Two major aspects of ion extraction modelling are evident. First, the generation processes of negative ion show some shortcomings: volume production seems low; wall production is large, but ions have wrong directions and/or large nonuniformity in current density; elastic scattering of wall generated ions into the extraction direction must compete with mutual neutralization. The detail of electrostatic field and ion trajectories depend strongly on the extraction shape.

Second, in the negative ion extraction case, the plasma sheath charge has to be negative on the extraction hole surface and positive on the nearby wall surface, which enhances beam aberration near hole edge.

In the next section, we recall some of the processes involved in negative ion generation and diffusion. In another section, the free-fall ion model is simplified[1] and the the plasma core-front model[2] is summarized; results of its implementation with a standard multi-physics code[3] are reported in the last section.

NEGATIVE ION COLLISIONS

In a negative ion source the gas density is of the order of $n_{gm} = 10^{20}$ atom/m^3 (corresponding to a maximum pressure $p_{gm} = 0.2$ Pa of H_2 at STP); consequently electron temperature is limited to few eV [4] and reduces below 1 eV near the plasma grid when a magnetic filter is present. Many collisional effects directly affects the H^- fate and source performance. These includes: (a) generation at a rate $\mathcal{G}_-$; (b) electron detachment in collision against H_2 and H; (c) charge transfer against H (which is mostly benefic, since it scatters the ion H^- towards extraction with a probability of the order of 50 %); (d) Coulomb collision against H^+ or H_3^+, with similar effects; (e) mutual neutralization with H^+ or H_3^+; (f) polarization scattering with H_2. To simplify notations, let assume the gas targets to be at rest, with mass m_t, charge i_t and let E_- be the incoming H^- kinetic energy, equal to $E_1 = 1$ eV in the examples. Note that the momentum cross sections $\sigma_b, \sigma_c, \ldots$ are more easily estimated and measured for $E_- \gg 1$ eV, so some extrapolation is here used. Let m_- and v_- be the H^- mass and speed, m_u the atomic mass unit; and $K = \sigma v_-$ the rate constants.

Electron detachment cross section σ_b is very modest (order of 1 Å^2) and Langevin polarization scattering cross section is moderately low (order of 30 Å^2). On the contrary, for resonant charge transfer between H and H^-, considering the estimate $\sigma_c = 225$ Å^2 at $E_- = 0.05$ eV [5] and the data (and formulas) for much larger E_-, we have

$$\sigma_c \cong \pi[a_0(c_0 + c_1 \mathrm{Log}[E_-/E_1] + c_2 \mathrm{Log}[E_-/E_1]^2)]^2 \quad (1)$$

with Log the decimal logarithm, a_0 the Bohr radius, the constants $c_0 = 13.62$, $c_1 = -2.135$ and $c_3 = -0.239$. This gives $\sigma_c = 163$ Å^2 at 1 eV, and $\sigma_c \gg \sigma_b$ in the E_- range of our interest (up to 20 eV).

Coulomb collision cross section σ_d is even larger:

$$\sigma_d = \pi b_0^2 [\tfrac{1}{4} + \tfrac{8}{\pi^2} \ln \Lambda], \quad b_0 = \frac{e^2 i_t (m_t + m_-)}{4\pi\epsilon_0 E_- m_t} \quad (2)$$

with $\ln \Lambda = 10$; this gives $\sigma_d = 2180$ Å^2 for H^+ and $\sigma_d = 970$ Å^2 for H_3^+.

For mutual neutralization [6] against H^+ and $E_- < 10$ eV, we use a simple power law $K_e \cong (E_-/E_1)^{-0.19} 1.2 \times 10^{-13}$ m^3/s (corresponding to a cross section $\sigma_e \cong 870$ Å^2 at $E_- = 1$ eV). Summing on all species, we estimate total recombination rate as $K_e n_+ n_-$.

THE PLASMA CORE-FRONT MODEL

When an ion produced at walls is scattered at a point z_i we consider that an ion is produced at z_i (with a large velocity spread) and an ion is of course absorbed. Let $\mathcal{G}$ be the generation rate of ions, that is the number of ions (multiplied by charge state i) produced per unit volume and time by ionization or by scattering. The ion density $n_i(\mathbf{z}) \equiv \varrho/e$ is $\int \mathrm{d}^3 z_i \mathcal{G}(\mathbf{z}_i) M/|\mathbf{v}(\mathbf{z}, \mathbf{z}_i)|$ where M takes into account motion and adsorption. In one-dimensional cases, if collisions are strong, $M = \frac{1}{2}\exp(|z - z_i|/\lambda_i)$ with λ_i the mean

* cavenago@lnl.infn.it

free path; when collisions are neglible, we set $M = 1$ for $z > z_i$ (with z-axis oriented in the prevailing motion direction), which is the free-fall 1D model [1].

Let $z = 0$ and $\phi = 0$ at the plasma electrode (see fig. 1), where ϕ is the electric potential; the lateral wall may have a small bias V_b while a large voltage V_e is applied to a puller electrode. To fix the ideas, let us consider the positive ion extraction case here (O^{2+}in detail), so that electrons are repelled by the extraction hole and may approach thermal equilibrium [7]; for simplicity we consider a one temperature distribution, so that electron density is

$$n_e = n_{e0}\exp(-u) \quad , \qquad u = -e(\phi - V_p)/T_e \tag{3}$$

where T_e is the temperature (in energy units), n_{e0} the density at plasma center where $\phi = V_p$, known as plasma potential. Note that $u = u_w = eV_p/T_e$ at plasma electrode and u_w will be determined by the solution (and balance of ion and electron currents). Poisson equation becomes:

$$-\triangle u = \lambda\left(\frac{n_e}{n_{e0}} - \frac{n_i}{n_{e0}}\right) \tag{4}$$

where $\lambda = 1/\lambda_D^2 = n_{e0}e^2/T_e\epsilon_0$ is the strength of nonlinear terms and λ_D the Debye length. The ion speed v_z is conveniently written as

$$v_z = \sqrt{\frac{2ei}{m_i}[\phi(z_i) - \phi(z)]} = c_s\sqrt{2}\sqrt{u(z) - u(z_i)} \tag{5}$$

with the Bohm speed $c_s = \sqrt{T_e/M}$ and the specific mass per charge $M = m_i/|i|$, where m_i is the ion mass. The generation density is parametrized as $\mathcal{G} = \nu_{io}\, n_{e0}\, g$ with $\nu_{io} = K_{io}n_g$ the ionization frequency (n_g primary gas density and K_{io} ionization rate constant) and g a form factor. Precisely $g = (n_e/n_{e0})^\gamma = \mathrm{e}^{-\gamma u}$ with $\gamma = 1$. The cases $\gamma = 0$ and $= 2$, as well as $M = (z_i/z)^\beta$, are also of some interest[8]. The ratio $n_i(z)/n_{e0}$ becomes a canonical integral expression

$$\frac{\nu_{io}}{\sqrt{2}c_s}\int_{z_p}^{z}\frac{\mathrm{d}z_i g(z_i)}{\sqrt{u(z) - u(z_i)}} = \int_0^s \frac{\mathrm{d}s_i g(s_i)}{\sqrt{u(s) - u(s_i)}} \equiv I(u) \tag{6}$$

changing variable to $s = (z - z_p)/L$, with z_p the plasma center. The length $L = \sqrt{2}c_s/\nu_{io}$ is the order of magnitude of plasma length needed to produce enough ions.

In typical simulation programs[9], note that n_i has to be determined by a sum of particle trajectories starting at user assigned positions; to obtain consistency, the electron charge density is empirically corrected as $n_e = n_i\alpha_p\exp(-u)$ with $0 < \alpha_p < 1$ an input parameter to adjust the V_p user guess. Other simulation programs[10, 11] use $en_i = k_f\left[(V_p - \phi)^2 + V_I^2\right]^{-1/4}$ or similar, with k_f determined from measured extracted ion currents, V_p guessed as before and $V_I \ll V_p$ a cutoff to avoid zero division at $V_p = \phi$. While eq. 6 prevents this problem and proves that $u_{,s} > 0$ for $s > 0$, its application and generalization to real 2D geometries is a difficult task. With u and s as variable, from eq. 4 the complete plasma equation is[1, 8]:

$$\tfrac{1}{2}\alpha^2\frac{\partial^2 u}{\partial s^2} = I(u) - \exp(-u) \quad , \quad \alpha = \frac{\sqrt{2}\lambda_D}{L} \ll 0.01 \tag{7}$$

where the lefthand side is a small perturbation only for $u \ll u_{break} \cong 0.854$; this is called the plasma regime, where $s(u) = s_0(u) + \alpha^2 s_p(u) + \ldots$. In the sheath regime $u \gg u_{break}$ the Child solution $s \propto u^{3/4}$ is retrieved, and the intricate intermediate regimes are described elsewhere[7].

We call the region $s \le s_a \equiv s(u_a)$ the plasma core, whose boundary values or reference values:

$$u_a = \tfrac{1}{4}\,, \quad s'_a \equiv s'(u_a)\,, \quad u'(s_a) = 1/s'_a\,, \quad u_m = \tfrac{1}{12} \tag{8}$$

can be computed analytically, and therefore plasma core does not need to be included in simulation; u_m is the average of u in plasma core. Thickness of the remaining plasma region, called the front plasma, can be easily estimated as $L(s_w - s_a)$ and will be numerically solved as a free boundary problem, subject to condition eq. 8. Here $s_w \equiv s(u_w)$; initial estimate of s_w and u_w from known 1D tables is standard[8]. Typically, $s_a \cong 0.30$ and $s_w = 0.5 \pm 0.1$ and $u_w = 5 \pm 1$. The main integral $I(u)$ divides into two parts $I(u) = I_1(u, u_a) + I_2(u, u_a)$ for $u \ge u_a$, defined as

$$I_1 = \int_0^{s_a}\frac{\mathrm{d}s_i g(s_i)}{\sqrt{u(s) - u(s_i)}}\,, \qquad I_2 = \int_{s_a}^{s}\frac{\mathrm{d}s_i g(s_i)}{\sqrt{u(s) - u(s_i)}} \tag{9}$$

It can be proven $I_1 = I_{10} + (\alpha^2/\pi)I_{12} + O[\alpha^2]$, where

$$I_{10} = \frac{2}{\pi}\left(\mathrm{e}^{-u}\mathrm{Asin}\sqrt{\frac{u_a}{u}} + \sqrt{u_a(u - u_a)}\sum_{j=0} u_a^j b_j f_j^b(u)\right) \tag{10}$$

with $f_0^b = (1 - \mathrm{e}^{-u})/u$, $f_1^b = (1 - u - \mathrm{e}^{-u})/u^2$ and so on. We keep terms up to $b_0 = 1$, $b_1 = 2/3$, $b_2 = 1/2$ for 10^{-5} accuracy. Expression for I_{12} is similar.

After a change of variable from s_i to $u_i = u(s_i)$, the integral I_2 can be approximately divided in three terms,

$$I_2 = \frac{j_F}{\sqrt{u - u_c}} + I_{2L} + I_{2H} \qquad j_F = \int_{s_a}^{s}\mathrm{d}s_i g(s_i) \tag{11}$$

where u_c is a sort of central (or average) value between u_a and u, chosen as $u_c(u) = u_\infty + [a/(u + b)]$, with $u_\infty = 0.592$, $a = -2(u_\infty - u_a)^2$, $b = 2u_\infty - 3u_a$. Moreover, note that j_F is the ion current produced in the frontal plasma (divided by $en_{e0}c_s\sqrt{2}$), and

$$I_{2H} = \int_{u_c}^{u}\mathrm{d}u_p\, g(u_p)\left(\frac{1}{\sqrt{u - u_p}} - \frac{1}{\sqrt{u - u_c}}\right)\left.\frac{\partial s}{\partial u}\right|_{u_p} \tag{12}$$

and similarly for I_{2L}, but with integration range $[u_a, u_c]$. From series expansion of $s_{,u}$ at $u_p = u$ we get $I_{2H} \cong I_{21}^H u_{,s}^{-1} - I_{22}^H u_{,ss}u_{,s}^{-3} + \ldots$; while I_{2L} estimate is more intricate, but smaller.

Now, as a first generalization to j_F definition eq. 11, we add deionization losses (with frequency ν_m^d) and transverse

diffusion in an uniform axial magnetic field B_0, with the approximation of frozen transverse motion:

$$\frac{\mathrm{d}j_F}{\mathrm{d}z} = S(j_F) \equiv \frac{g}{L} - \frac{j_F}{L_a} + \frac{1}{L_d}\frac{\partial^2 j_F}{\partial y^2} \qquad (13)$$

where $L_a = v_z/\nu_m^d$ is the absorption length, $L_d = 2v_z/R\nu_m$ is the transverse diffusion length, ν_m is the total (momentum) collision frequency and $R = 1/(1 + (\Omega_i/\nu_m)^2$ is factor depending on the ion cyclotron frequency $\Omega_i = eB_0/M$. With the finer approximation of a laminar transverse motion like $y = y_0 a(z)$, we have

$$\frac{\partial j_F}{\partial z} + y\frac{a'(z)}{a(z)}\frac{\partial j_F}{\partial y} = -\frac{a'(z)}{a(z)} j_F + S(j_F) \qquad (14)$$

Note that halo space charge is still missing here. Finally, particle motion equations in scaled variables are

$$\frac{\partial^2 y}{\partial \ell^2} = u_{,y} + \tilde{k}_A(y_0 - y) \quad , \quad \frac{\partial^2 z}{\partial \ell^2} = u_{,z} \qquad (15)$$

where $\ell = tc_s$ is a length and $\tilde{k}_A = \frac{e^2 B_0^2}{MT_e} = \left(\frac{\Omega_i}{c_s}\right)^2$. In cylindrical symmetry, the first equation changes to

$$\frac{\partial^2 y}{\partial \ell^2} = u_{,y} + \tilde{k}_A \frac{(y_0^4 - y^4)}{4y^3} \qquad (16)$$

NUMERICAL SIMULATIONS

A multi-physics code [3] can solve Eq. 4 for u, when it is controlled by scripts (now named 'planar2init.m' and so on), specifying the nonlinear terms as eq. 10. Together with u we can solve eq. 13, which is still in PDE form; u and j_F are fields of a coupled PDE system. A third field arises from the free boundary eq. 8. For numerical stability reasons, script slowly solves this equation iteratively, allowing a limited boundary deformation; in the same iteration, u_w value is refined. Some ion tracing is done at the end. In total, we have about 50 kbytes of application scripts[2], running in about 150 s on a 3.4 GHz P4 computer. As evident in eq. 8 and 11, the particle start condition is determined (approximately) in the plasma core-front model. In fig. 1 note the aberration of outer rays, and the distortion of $\phi_{,z}$ near $(0, r_h)$, originating the halo.

On the contrary, particle tracing codes require the specification of the particle starting conditions. With a careful choice of proton and electron starting conditions, a self consistent solution for the electrostatic potential ϕ can be found with a PIC code (see fig 2), from which the plasma potential V_p is obtained. Negative ions may then be added as a test beam, since their contribution to the space charge is small. Fig 2 also emphasizes that the aberrations of the H^- beam due to the PG geometry and the strong field gradients at extraction are even larger than the positive ion case. Work to optimize the PG shape and to include the smoothing effects of collision on the extracted beam is in progress. Also we plan to export eq. 8 particle start conditions to this and other codes.

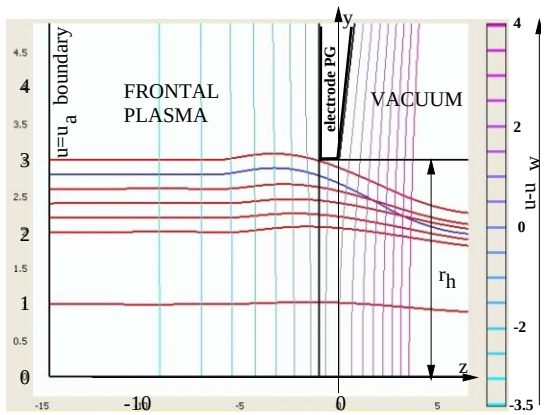

Figure 1: O^{2+} trajectories (thick lines) from a tenuous plasma ($\lambda_D = 1.69$ mm, $L = 30$ mm): region boundaries (thick lines); equipotential of u and ϕ (thin lines); dimension in mm; $u_w = 4.21$ and extraction potential $u_e = 82.56$, that is 1.3 times the Child voltage. Deformation of $u = u_a$ boundary (about 0.1 mm) is not plotted.

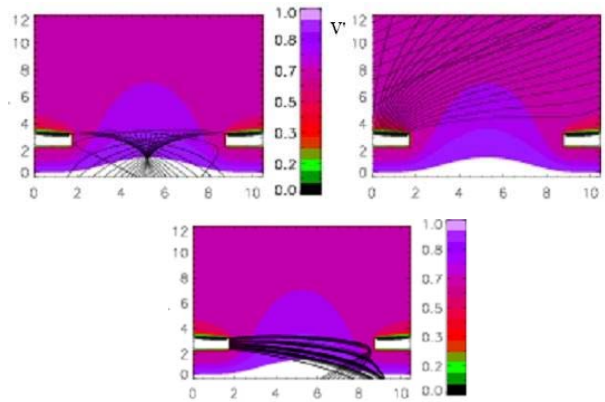

Figure 2: Example of H^- extraction from plasma for several position of the generation site. Ion trajectories in black; scaled potential $V' = \phi/V_p$ in color (or gray tones). Left panel: start in volume plasma near PG; right panel: start on the PG backside; lower panel: start on the PG extraction hole border. Dimension in mm, with $d = 10$ mm.

REFERENCES

[1] L. Tonks, I. Langmuir, Phys. Rev. **34** (1929), 826

[2] M. Cavenago, 2006, unpublished.

[3] http://www.comsol.com and *Comsol 3.2*, 2005

[4] R. Zorat and D. Vender, J. Phys. D, 33 (2000), 1728

[5] S. Sinha , J. N. Bardsley, Phys. Rev. **A14** (1976), 104

[6] J. Moseley et al., Phys. Rev. Lett., **24** (1970), 435

[7] K. U. Riemann et al., Plasma Phys. Control. Fusion **47** (2005), 1949

[8] S. A. Self, Phys. Fluids **6** (1963), 1762

[9] P. Spadtke, Rev. Sci. Instrum., **75**, 1643 (2004)

[10] R. Becker, Rev. Sci. Instrum. 75 (2004), 1687

[11] M. Cavenago, A. Galata, Radiation Effects and Defects in Solids, **160** (2005), 499